The role of linker DNA in chromatin fibers

Brouwer, T.B.

Chapter 2

Methods for Unravelling DNA organization with single-molecule Force Spectroscopy using Magnetic Tweezers

Genomes carry the genetic blueprint of all living organisms. Their organization requires strong condensation as well as carefully regulated accessibility to specific genes for proper functioning of their hosts. The study of the structure and dynamics of the proteins that organize the genome has benefited tremendously from the development of single-molecule force spectroscopy techniques that allow for real-time, nanometer accuracy measurements of the compaction of DNA and manipulation with pico-Newton scale forces. Magnetic tweezers in particular have the unique ability to complement such force spectroscopy with the control over the linking number of the DNA molecule, which plays an important role when DNA organizing proteins form or release wraps, loops and bends in DNA. Here, we describe all the necessary steps to prepare DNA substrates for magnetic tweezers experiments, assemble flow cells, tether DNA to a magnetic bead inside flow cell and manipulate and record the extension of such DNA tethers. Furthermore, we explain how mechanical parameters of nucleo-protein filaments can be extracted from the data.

This chapter is based on: Brouwer T. B., Kaczmarczyk A., Pham C., van Noort S. J. T.: Unravelling DNA organization with single-molecule Force Spectroscopy using Magnetic Tweezers, **Bacterial Chromatin**, Humana Press, New York, NY, 2018: 317-349.

2.1 Introduction

2.1.1 Chromatin organization by DNA-binding proteins

Genomes carry the genetic blueprint of all living organisms. Their organization requires strong condensation in a structure called chromatin, as well as carefully regulated accessibility to genes in chromatin for proper functioning of their hosts. The organization of chromatin is carried out by a large group of proteins that vary in abundance, structure and function. Different kingdoms of life have evolved to implement different solutions for a compact, but dynamic organization of chromatin. Nonetheless, many of the involved proteins share common mechanisms to deform the DNA by inducing kinks, bends, wraps and loops in the DNA trajectory. Examples of common DNA organizing proteins are histone proteins found in eukaryotes and in Archaea and smaller and more diverse proteins like HU, integration host factor IHF and histone-like nucleoid-structuring protein H-NS in prokaryotes [1].

For a mechanistic understanding of the function of these proteins, required for a robust comprehension of chromatin-associated processes such as transcription, a detailed knowledge of the kinetics of DNA binding, as well as the mechanical consequences of their binding to DNA is needed. In fact, there is a tight relationship between DNA conformation and its interaction with proteins: wrapping of DNA around proteins results in condensation of the DNA, both by bringing together the ends of the DNA and by inducing supercoiling in the surrounding DNA, which results in additional condensation by plectoneme formation. DNA supercoiling, induced by externally applied torque, will facilitate the binding of proteins that wrap or bend the DNA with similar chirality. Force and extension play similar related roles: some proteins induce stretching of DNA upon binding. Pre-stretching of DNA can facilitate binding or function of these proteins, making force an important parameter in the study of nucleo-protein filaments [2].

DNA forms the common thread in chromatin organization, and it is informative to gather and compare mechano-chemical experimental data on chromatin organization by different proteins and from different species, to gather a comprehensive picture of DNA organization. In terms of DNA mechanobiology, as well as from an evolutionary perspective, it is highly desirable to establish a physical understanding of chromatin organization throughout the kingdoms of life. In this chapter, we present protocols to set up single-molecule force spectroscopy experiments on DNA tethers interacting with a variety of chromatin proteins. Although some examples stem from studies of eukaryotic proteins, it is our experience that the methods for sample preparation, execution of the experiments and data analysis are similar, and we provide protocols that can be used to study bacterial chromatin, as well as other nucleoprotein complexes.

2.1.2 Magnetic tweezers

Magnetic Tweezers (MT) can probe the mechanical response of individual biomolecules to applied force and twist. The first MT experiments have been instrumental in understanding the mechanical behavior of bare DNA [3–5]. Since then, mechanical and structural properties of more complex biomolecules and DNA-protein complexes have been studied [6–11]. MT are especially suitable to this end since they require limited hardware investments, uniquely control both force and linking number, and have a relatively high throughput compared to optical tweezers, the most common alternative single-molecule force spectroscopy technique. Recent developments are an increase in maximum force to beyond the overstretching force for DNA [8, 12, 13], multiplexing capabilities, such that hundreds of molecules can be measured in parallel [14, 15] and freely orbiting magnetic tweezers (FOMT) [16] or magnetic torque tweezers (MTT) [17], that allow for (partial) relief of twist or direct torque measurement. Another advance is the replacement of permanent magnets by electromagnets in electromagnetic tweezers [5, 18]. Since there are no moving parts in electromagnetic tweezers, the only factor limiting the speed of the experiments is the viscous drag of the magnetic beads themselves. Finally, combinations with (single-molecule) fluorescence have been reported [19–22]. These modern variations of the technique require similar sample preparation protocols and can be seen as extensions of typical MT experiments.

A typical MT experiment involves a single DNA molecule tethered between a paramagnetic bead and a functionalized glass slide. The three-dimensional position of the bead is recorded in time by video microscopy and extracted by image processing. The bead can be manipulated by translation or rotation of a pair of magnets that are held above the tether. The force and torque that are exerted on the paramagnetic bead result in a restoring force and torque in the tethered molecule, which provides insight into the structure of the tether.

2.1.3 Measurement schemes

MT can be operated in several measurement schemes. Traditionally, the magnet is fixed in a preset position during a measurement, resulting in a constant force during the experiment. For bare DNA, such a constant force measurement not only accurately reveals the extension of the tether, one can also directly calculate the force by quantification of the lateral movements of the bead [4]. Application of the equipartition theorem yields that the force must equal the product of thermal energy and extension, divided by the variance of the lateral fluctuations (*see* section 3.7). Repeated measurements at different magnet positions yield a calibration of the force as a function of the magnet position [4, 23–26], which typically follows a mono- or bi-exponential decay [25]. The same measurement also provides an accurate map of the force-extension relation

of DNA, which can be described by a Worm-like Chain (WLC) model. For transient protein-DNA interactions, a constant force experiment can directly reveal changes in extension of the tether upon flushing the protein solution in or out [27–29].

Having established a force calibration relation, one can revert to dynamic force spectroscopy, in which the extension of the tether is monitored during the repositioning of the magnet [30]. Such a measurement scheme aids in revealing the force dependence of structures that may rupture or dissociate when increasing forces are applied. For instance, we have noticed that histone proteins readily dissociate when chromatin fibers are exposed to forces exceeding several pN [11].

Next to shifting the position of the magnets with respect to the tethered bead, the magnets can be rotated around the axis of the tether. Since the torque on the bead is proportional to the strength of the magnetic field (*see* **Note 1**), and is typically much larger than the opposing torque provided by the DNA tether, the bead will immediately follow the rotation of the magnets. This can lead to accumulation of twist in the tether, if the twist is not relieved by swiveling around the bond between the tether and bead or surface, or by swiveling around a nick in the DNA. Constraining the rotation of the DNA ends requires more than one chemical bond between the DNA strand and the bead or surface, which can be achieved by introducing multiple affinity tags in the DNA ends. Such a DNA substrate allows for direct control of the linking number of the topological domain formed by the bead and the surface. Here, we describe the preparation of both torsionally constrained and torsionally free DNA substrates, allowing for a broad spectrum of applications.

Controlling the linking number of the DNA tether opens up a range of measurement schemes. At constant twist, force-extension measurements can be done in a similar fashion as with torsionally unconstrained DNA. Any twist-stretch coupling will be evident in the force-extension curve. Protein-induced (un-)wrapping will accumulate, which may affect the binding of subsequent proteins. A torsionally constrained tether can be pre-twisted before force spectroscopy experiments, to probe the chiral properties of the tether over a wide range of linking numbers [31]. The mechanical response of the tether to torque can also be measured directly by twisting the tether under constant force. In conclusion, a wide variety of single-molecule manipulation schemes is available with MT force spectroscopy.

2.1.4 Data analysis

The mechanical properties of DNA provide a reference for data analysis of nucleo-protein filaments. The extension of DNA as a function of force can be described accurately by the WLC model [32]. At forces larger than 10 pN, the extensible WLC model provides a better fit [32, 33]. DNA extension

as a function of twist requires a more elaborate analysis, using numerical methods, due to the coexistence of three conformations, *i.e.* twisted, melted and plectonemic DNA [31]. However, for force and twist regimes where only two of these states prevail, analytical solutions exist [34]. In general, it is important to make sure that the force-extension curves of bare DNA, under conditions relevant for studying chromatin, fit well to these models, prior to the study of more advanced structures, as protein-induced changes in extension can be difficult to interpret without proper reference.

Wrapping, bending, twisting or deforming DNA otherwise, will result in a change in extension of the tether that may depend on force and twist. In a force-extension curve, this may lead to a change in persistence length, contour length, stretch modulus and/or twist persistence length. In the data analysis part of the methods section, we review some models that can be fitted to extract these parameters, as well as more dynamic methods to extract the kinetics of protein binding. Below, we describe in detail how to make DNA substrates suitable for MT. Note that many variations of DNA substrates exist that the reader can adapt to specific needs. We report a detailed protocol for the assembly of DNA tethered beads in a flow cell, ready for measurements, and share some typical procedures for data analysis. These should provide a solid foundation to study chromatin at the single-molecule level with MT.

2.2 Materials

2.2.1 Stock solutions

All aqueous buffers are prepared with Milli-Q water and stored at 4°C.

- *Measurement buffer*: 10 mM HEPES pH 7.5, 100 mM NaCl, 10 mM NaN_3 (sodium azide), 0.2% Bovine Serum Albumin (BSA) (heat shock fraction, pH 7, $\geq$ 98%), 0.1% TWEEN 20 (*see* **Note 2**).
- *Passivation buffer*: 10 mM sodium azide, 3.6% BSA and 0.1% TWEEN 20 (*see* **Note 2**).

2.2.2 Isolation of DNA plasmids

- Desired DNA plasmid (*see* **Note 3**)
- XL1-Blue competent cells
- Heat block, such as the Eppendorf ThermoMixer
- Orbital shaker
- Microcentrifuge, such as the Eppendorf 5424R
- Lysogeny broth (LB) medium (*see* **Note 4**)
- LB agar plates (*see* **Note 4**)
- 500 mL Erlenmeyer flask
- DNA plasmid isolation kit, such as the NucleoBondXtra Midi kit

2.2.3 Digestion and labeling of DNA

- Isolated DNA plasmid (*see* **Note 3**)
- Restriction enzymes (*see* **Note 3**)
- Reaction buffer for digestion
- DNA purification kit, such as the Wizard SV Gel & PCR cleanup kit
- Spectrophotometer for micro volume quantitation of nucleic acids, for instance the BioDrop µLITE
- Agarose for DNA/RNA-electrophoresis
- Horizontal electrophoresis system

- dNTPs (100 mM)
- DNA Ladder
- Ethidium Bromide (10 mg/mL)
- Klenow fragment
- Reaction buffer for Klenow Fragment
- Digoxigenin–labeled ddUTP (1 mM)
- Biotin–labeled ddUTP (1 mM)
- DNA plasmid as a template for DNA handles (*see* **Note 3**)
- Forward primer to construct DNA handles (*see* **Note 3**)
- Backward primer to construct DNA handles (*see* **Note 3**)
- T4 DNA Ligase
- Reaction buffer for T4 DNA Ligase
- DNA PCR kit, such as the FastStart Taq DNA Polymerase kit
- Digoxigenin–labeled dUTP (1 mM)
- Biotin–labeled dUTP (1 mM)
- Sodium dodecyl sulfate (SDS) $\geq$ 98.5% (GC)
- PCR Thermal Cycler, such as the Bio-Rad T100
- UV Transilluminator, such as the Bio-Rad UVT 2000
- Imaging system for visualization of electrophoresis gels, such as the ChemiDoc Imaging Systems

2.2.4 Flow cell assembly

- High-precision crossover tweezers
- Carbon steel scalpel
- N_2 spray gun
- 2-Propanol
- Custom-built aluminum flow cell body

- Custom-built Perspex mold
- Embossing Tape (9 mm)
- Cover slip 24 × 40 mm (#1.5 thickness)
- Cover slip 24 × 60 mm (#1.5 thickness)
- PDMS kit, for instance the Sylgard 184 Silicone Elastomer Kit
- FEP Tubing (1/16" outer diameter × 0.020" inner diameter)
- Flexible electrical wire (of approximately 0.02" outer diameter)
- Fitting nut for 1/16" outer diameter tubing
- Ferrule for 1/16" outer diameter tubing
- Vacuum controller
- 5 mL syringe
- M4 bolts
- Ultrasonic cleaning bath
- Glass staining trough
- 100 mL glass beaker
- Microscope slide (75 × 26 × 1 mm)

2.2.5 Bead-tether assembly

- DNA substrate (torsionally constrained or torsionally free)
- Magnetic rack for bead separation
- Streptavidin – coated paramagnetic beads (*see* **Note 5**)
- Nitrocellulose (0.1% in amyl acetate)
- Anti-digoxigenin (AD)
- 1 mL syringe
- 18G single-use needle
- Flexible tubing (0.8 mm inner diameter / 0.8 mm wall)
- Peristaltic pump (which can exert flow rates of approximately 50 µL / minute)

2.2.6 Microscope

- Microscope objective (flat-field, NA = 1.3, 40×, oil immersion, field number 25)
- CMOS camera (25 Mpix, 8 bit, 30 fps, Camera Link – Full interface)
- Infinity-corrected tube lens (f = 200 mm)
- Kinematic pitch/yaw adapter
- LED-collimator (645 nm, 100 µW, 20mA)
- Frame grabber for Camera Link – Full interface
- Multi-core PC (*e.g.* 10-cores) with 32GB DDR3 memory
- *xyz* piezo stage (20 µm travel in *z*, 0.1 nm resolution)
- Cube magnets (N50 magnetized, 5 mm)
- Stepper motor controller (6-axis, 1-256 micro-steps)
- Hollow-shaft stepper motor (2-phase, NEMA 8)
- Two translation stages to mount objective and magnets (20 mm travel, 0.1 µm resolution)
- *xy* manual positioning stage (20 mm travel in *xy*, 65 mm aperture)
- Ø1" and Ø2" broadband dielectric mirrors (λ = 400 - 750 nm)

2.3 Methods

2.3.1 Isolation of DNA plasmids

1. Take 100 µL of XL1-Blue Competent Cells (at a concentration of approximately 3×10^8 cells / mL) from the -80°C freezer and let thaw on ice (*see* **Note 6**).

2. Add approximately 1.0 µL of the desired DNA plasmid (*see* **Note 7**) to the Eppendorf tube, gently mix and incubate on ice for a minimum of 30 minutes.

3. Heat-shock the sample for 90-120 seconds at 42°C by means of the thermomixer. Do not shake the sample or exceed the indicated time.

4. Place the tube back on ice for 60 seconds and add 900 µL of LB medium. Gently shake (240 rpm) and incubate the tube for 30-60 minutes at 37°C.

   item Centrifuge the tube for 60 seconds at 20,000 g, remove approximately 90% of the supernatant and re-suspend the sample.

5. Spread the sample on an LB agar plate containing the appropriate antibiotic (here: ampicillin) and incubate (upside down) at 37°C overnight.

6. Pick up one colony and put it into a 500 mL Erlenmeyer flask containing 250 mL LB medium and the appropriate antibiotic (here: ampicillin). Incubate on the shaker (320 rpm) at 37°C, overnight.

7. Isolate and purify the DNA plasmid DNA the NucleoBond® Xtra Midi kit (Macherey-Nagel) following the manufacturers' protocol.

2.3.2 Digestion and labeling of torsionally free DNA constructs

1. Digest the DNA plasmid by mixing the reagents listed in Table 2.1 in an Eppendorf tube and incubate at 37°C, overnight (*see* **Notes 8 and 9**).

2. Inactivate BsaI by incubating for 20 minutes at 65°C (*see* **Note 10**).

3. Purify DNA with Promega Wizard SV Gel & PCR cleanup kit following the manufacturers' protocol (*see* **Notes 11 and 12**). Determine the DNA concentration after purification by measuring A260 nm peak absorbance with the spectrophotometer and store a microliter of the reaction mixture for agarose gel electrophoresis.

4. Label one end of the digested DNA by mixing the reagents listed in Table 2.2 in an Eppendorf tube and incubate at 37°C, for 2 hours (*see* **Note 13**). The end concentration of (labeled) dNTPs should be 20 µM (*see* **Note 14**). Note that in this step the DNA is labeled with ddUTP rather than dUTP (*see* **Note 15**).

5. Purify DNA and store a microliter of reaction mixture for agarose gel electrophoresis.

6. Digest the DNA labeled in the previous steps with a single digoxigenin by mixing the reagents listed in Table 2.3 in an Eppendorf tube and incubate at 37°C, overnight.

7. Inactivate BseYI by incubating for 20 minutes at 80°C.

8. Purify DNA and store a microliter of reaction mixture for agarose gel electrophoresis.

pUC18 DNA plasmid (with 601-array) (2000 ng/µL)	20 µL	40 µg
NEBuffer (10× concentrated)	80 µL	–
Milli-Q water	696 µL	–
BsaI (10 U/µL)	4 µL	40 units
Total volume	**800 µL**	

Table 2.1
Composition of digestion reaction mixture I, used for preparation of the torsionally free construct.

BsaI-digested pUC18 DNA (with 601-array) (400 ng/µL)	50 µL	20 µg
Reaction buffer for Klenow Fragment (10× concentrated)	10 µL	–
Digoxigenin-11-ddUTP (1 mM)	2 µL	20 µM
dGTP (1 mM)	2 µL	20 µM
dCTP (1 mM)	2 µL	20 µM
Milli-Q water	24 µL	–
Klenow Fragment, LC (2 U/µL)	10 µL	20 units
Total volume	**100 µL**	

Table 2.2
Composition of labeling reaction mixture I, used for preparation of the torsionally free construct.

9. Label the second extremity of the DNA by mixing the reagents listed in Table 2.4 in an Eppendorf tube and incubate at 37°C, for 2 hours.

10. Purify DNA and store a microliter of reaction mixture for agarose gel electrophoresis.

11. Check the digestion reaction products by electrophoresis using a 1% agarose gel. Pre-stain the gel with ethidium bromide by diluting the stock 10,000× in the agarose solution before it cures (*see* **Note 16**). Load the gel with the products obtained at different steps of the labeling procedure, flanked by two DNA ladders. Load approximately 50-100 ng of DNA per lane. Run the gel in TBE buffer in a horizontal electrophoresis system for 1-2 hours at 90 mV or until bands are adequately separated. Visualize the electrophoresis gel in an imaging system adjusted for ethidium bromide staining.

2.3.3 Digestion and labeling of torsionally constrained DNA constructs

1. Digest the DNA plasmid by mixing the reagents listed in Table 2.5 in an Eppendorf tube and incubate at 37°C, overnight (*see* **Notes 8 and 9**).

Single-labeled pUC18 DNA (with 601-array) (200 ng/µL)	50 µL	10 µg
NEBuffer 3.1 (10× concentrated)	20 µL	–
Milli-Q water	128 µL	–
BseYI (5 U/µL)	2 µL	10 units
Total volume	**200 µL**	

Table 2.3
Composition of DNA plasmid digestion reaction mixture II, used for preparation of the torsionally free construct.

BseYI-digested single-labeled pUC18 DNA (with 601-array) (150 ng/µL)	50 µL	7.5 µg
Reaction buffer for Klenow Fragment (10× concentrated)	10 µL	–
Biotin-16-ddUTP (1 mM)	2 µL	20 µM
dCTP (1 mM)	2 µL	20 µM
Milli-Q water	32.25 µL	–
Klenow Fragment, LC (2 U/µL)	3.75 µL	7.5 units
Total volume	100 µL	

Table 2.4
Composition of labeling reaction mixture II, used for preparation of the torsionally free construct.

The two enzymes are used at the same time.

2. Inactivate restriction enzymes by incubating for 20 minutes at 80°C.

3. Separate the digestion products by electrophoresis using a 1% agarose gel. Pre-stain the gel with ethidium bromide by diluting the stock 10,000× in the agarose solution before it cures (*see* **Note 16**). Load the digested DNA in a large slot, obtained by using 1.0 mm comb and merging several lanes (with tape), flanked by two DNA ladders. Before loading, add SDS to an end concentration of 0.5% (*see* **Note 17**).

4. Image the gel on the UV transilluminator to locate the bands of interest. Minimize the time on the UV transilluminator (*see* **Note 18**). Use a scalpel to cut the digested DNA from the gel, to separate the construct of interest from the DNA backbone.

5. Purify the digested DNA from gel with the Promega Wizard SV Gel & PCR cleanup kit following the manufacturers' protocol (*see* **Note 19**).

6. Construct two sets of handles with multiple biotin or digoxigenin affinity tags by polymerase chain reaction (PCR) (*see* **Notes 20 and 21**). Mix the reagents listed in Table 2.6 in two separate Eppendorf tubes and place them in the thermal cycler. Use the PCR program depicted in Table 2.7

pUC18 DNA plasmid (with 601-array) (2000 ng/µL)	50 µL	100 µg
NEBuffer 3.1 (10× concentrated)	200 µL	–
Milli-Q water	1720 µL	–
BsaI (10 U/µL)	10 µL	100 units
BseYI (5 U/µL)	20 µL	100 units
Total volume	**2000 µL**	

Table 2.5
Composition of the reaction mixture for digestion of the DNA plasmid for the torsionally constrained construct.

and store the tubes at 4°C. Here, the DNA is labeled with dUTP rather than ddUTP (*see* **Notes 15 and 22**).

7. Digest the biotin PCR product with BsaI and the digoxigenin PCR product with BseYI by mixing the reagents listed in Table 2.8 in two different Eppendorf tubes and incubate at 37°C, overnight.

8. Inactivate restriction enzymes by incubating for 20 minutes at 80°C.

9. Purify digested PCR products with the Promega Wizard SV Gel & PCR cleanup kit following the manufacturers' protocol (*see* **Notes 12 and 23**).

10. Ligate the digested DNA plasmid with the digested PCR products containing the multiple biotin or digoxigenin affinity tags. The digested DNA and PCR products are mixed in equimolar ratio. Mix the reagents listed in Table 2.9 in an Eppendorf tube and incubate at 4°C, overnight. Before ligase is added, store a microliter of reaction mixture for agarose gel electrophoresis (*see* **Notes 24 and 25**).

11. Inactivate T4 ligase by incubating for 20 minutes at 65°C.

12. Purify ligated DNA, elute at least two times (*see* **Note 26**). Store a microliter of reaction mixture for agarose gel electrophoresis.

13. Check the ligation reaction by electrophoresis using a 1% agarose gel. Pre-stain the gel with ethidium bromide by diluting the stock 10,000× in the agarose solution before it cures (*see* **Note 16**). Load the gel with unligated and ligated reaction products, flanked by two DNA ladders. Load approximately 50-100 ng of DNA per lane. Run the gel in TBE buffer in a horizontal electrophoresis system for 1-2 hours at 90 mV or until bands are adequately separated. Visualize the electrophoresis gel in an imaging system adjusted for ethidium bromide staining.

Template pUC18 DNA plasmid (100 ng/µL)	1 µL	100 ng
FastStart Taq DNA Polymerase (5 U/µL)	0.5 µL	2.5 units
Forward primer to construct DNA handles (10 µM)	1 µL	100 nM
Backward primer to construct DNA handles (10 µM)	1 µL	100 nM
PCR Reaction Buffer + $MgCl_2$ (10× concentrated)	10 µL	–
dNTP (10 mM)	1 µL	100 µM
Biotin-16-dUTP (1 mM) / Digoxigenin-11-dUTP (1 mM)	1 µL	10 µM
Milli-Q water	84.5 µL	–
Total volume	**100 µL**	

Table 2.6
Composition of the PCR mixture for production of DNA handles for the torsionally constrained construct.

Step	**Temperature (°C)**	**Time (s)**	**Function**
1	95	240	Melt the DNA
2	95	30	Melt the DNA
3	50	45	Anneal the primer to the ssDNA
4	72	60	Elongation by DNA polymerase
5	72	300	Fill in any protruding ends

Table 2.7
The PCR program to produce the DNA handles. Steps 2–4 are cycled 30 times.

Multi-bio. PCR product / Multi-dig. PCR product (200 ng/µL)	100 µL	20 µg
NEBuffer 3.1 (10× concentrated)	100 µL	–
Milli-Q water	798 µL / 796 µL	–
BsaI (10 U/µL) / BseYI (5 U/µL)	2 / 4 µL	20 units
Total volume	**1000 µL**	

Table 2.8
Composition of the digestion reaction mixture for generation of the DNA handles of the torsionally constrained construct.

Digested pUC18 DNA (with 601-array) (100 ng/µL)	300 µL	30 µg
Digested multi-biotin PCR product (100 ng/µL)	50 µL	5 µg
Digested multi-digoxigenin PCR product (100 ng/µL)	50 µL	5 µg
T4 DNA Ligase Reaction Buffer (10× concentrated)	80 µL	–
Total volume	315 µL	–
T4 DNA ligase (400 U/µL)	5 µL	2000 units
Total volume	**800 µL**	

Table 2.9
Composition of the ligation reaction mixture to produce the torsionally constrained construct.

2.3.4 Flow cell assembly

1. Mix the two components of the PDMS in a ratio 10 : 1 (viscous monomer : non-viscous elastomer), approximately 2 mL per flow cell. Mix carefully and thoroughly (*see* **Note 27**). Degas the PDMS by keeping the mixture at 300 mBar for 2 hours using the vacuum controller.

2. Clean the Plexiglas molds and aluminum flow cell body with 2-propanol and Milli-Q water, and dry in a stream of N_2. On the mold, place a strip of embossing tape which shapes the channel. Using a needle, puncture two holes through the tape, which are used to pass through two electrical wires. Place the 24×40 mm cover slip into the aluminum body. For the in- and outlet of the flow cell, insert two pieces of 3 cm flexible electrical wire into approximately 10 cm of FEP tubing. Assemble the fitting nut and ferrule onto the tubing. Mount the tubing onto the side of the flow cell. Guide the tubing through the side of the flow cell and secure the fitting nut tightly. Guide the electrical wire through the Plexiglas molds into the tubing. Fix the flow cell body and mold with the M4 bolts. The physical assembly of the flow cells is illustrated in Figure 2.1.

3. Using a 5 mL syringe, slowly flow the degassed PDMS into the flow cell. Prevent bubbles as much as possible. Cure the flow cells at 65°C for at least 5 hours (up to overnight).

4. Remove electrical wires, creating connection channels in the PDMS to the in- and outlet of flow cell. Remove the Perspex mold. Use a scalpel to widen the channel in the flow cell to approximately 10 mm. Make sure the channel is connected to the in- and outlet of the flow cell.

5. Put multiple 24×60 mm cover slips in a glass staining trough and sonicate in ultrasonic cleaning bath for 15 minutes in 2-propanol. Dry the cover slips in a stream of N_2 or allow the cover slips to dry in air.

6. Put 5 mL of 0.1 % nitrocellulose in amyl acetate in a 100 mL glass beaker. Place a clean microscope object slide vertically in the solution. Using reversed tweezers, place one of the sonicated cover slips into the beaker directly next to the microscope slide. Capillary forces will fill the gap between the slides with nitrocellulose solution and will quickly coat the cover slip (*see* **Note 28**).

7. Once the gap between the cover slip and the object slide is filled, use reversed tweezers to carefully slide the cover slip from the object slide. Dry the cover slip in a stream of N_2. Place the cover slip with the nitrocellulose-coated side at the bottom of the flow cell, sealing the flow channel or store the coated cover slip for later use.

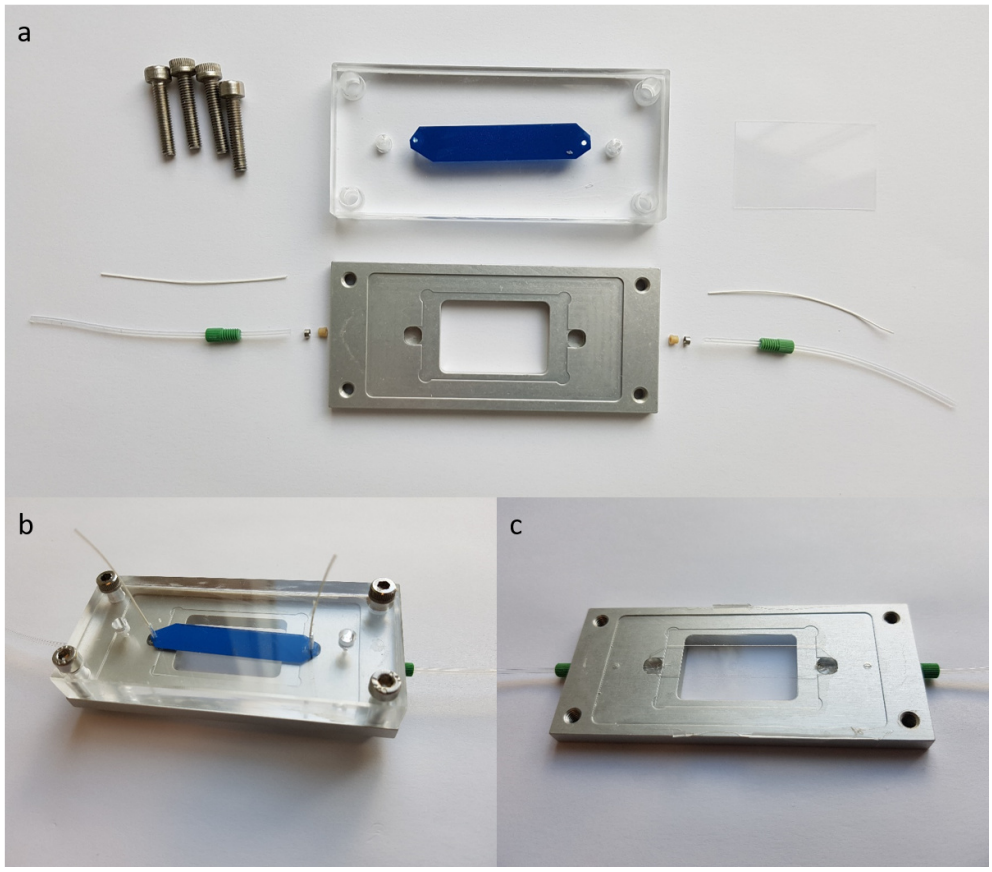

Figure 2.1
The assembly of the custom-built flow cells is a three-step process. a) Tubes and slides are assembled. The 24 × 40 mm glass slide is placed in the designated cavity of the aluminum body. Electric wire is inserted into the FEP tubing and guided upward through the mold. b) After mounting the Perspex mold, the assembled flow cell is ready for casting PDMS. c) Once the PDMS is cured, the electric wire and mold can be removed and the flow cell is covered by a 24 × 60 mm biochemically functionalized glass slide.

2.3.5 Bead-tether assembly

1. Connect the tube on one side of the flow cell to an empty syringe using a short length of flexible silicone tubing and a needle. Carefully flush the flow cell with 1 mL of Milli-Q water, incubate for approximately 30 seconds.

2. Replace the Milli-Q water with 300 µL of 10 ng/µL anti-digoxigenin solution. Incubate at 4°C for 2 hours.

3. Passivate the flow cell by flowing in 1 mL of passivation buffer. Incubate

at 4°C overnight (*see* **Note 29**).

4. Flush the flow cell with 1 mL of measurement buffer.

5. Dilute 1 ng of DNA in 500 µL measurement buffer. Flush the flow cell with DNA and incubate at room temperature for 10 minutes (*see* **Note 30**).

6. Vortex and wash the 1 µg/µL paramagnetic beads in Milli-Q water by means of the magnetic rack and dilute 1 µL of paramagnetic beads in 500 µL measurement buffer. Flush the flow cell with beads and incubate at room temperature for 10 minutes (*see* **Note 31**).

7. Slowly flush out the excess beads from the flow cell with 500 µL of measurement buffer using a peristaltic pump at 500 µL/minute (*see* **Note 32**).

8. The flow cell is now ready for measurements on bare DNA or incubation with DNA binding proteins.

2.3.6 Initial bead selection and height calibration

1. Position the magnets at such a distance that force is negligible. In our setup, depicted in Figure 2.2 (*see* **Note 33**), we position the magnets 10 mm above the sample, resulting in a force lower than 0.05 pN.

2. Place the flow cell containing the (pre-incubated) sample onto the microscope.

3. Put the beads in focus using the objective mounted onto the stepper motor. With the piezo stage, move the objective 10 µm above focus so distinct diffraction rings appear around the beads (*see* **Note 34**).

4. Select regions-of-interest (ROIs) of 150 × 150 pixels containing single, isolated beads (*see* **Note 35**).

5. Identify an immobile bead as reference bead, and use this bead for phase calibration. Move the bead 20 µm in z while cross-correlating the bead images with a set of computer-generated reference images. Calibrate the phase of the cross-correlation peak with bead height. When there are no immobile beads in the field of view, phase calibration can also be done at an intermediate force, *i.e.* 1 pN, to reduce the thermal fluctuations of the tethered bead while keeping the tether intact.

6. Once the measurement plane is set and phase calibration is complete, assign the ROIs to tethered beads (manually or by a bead-finding algorithm).

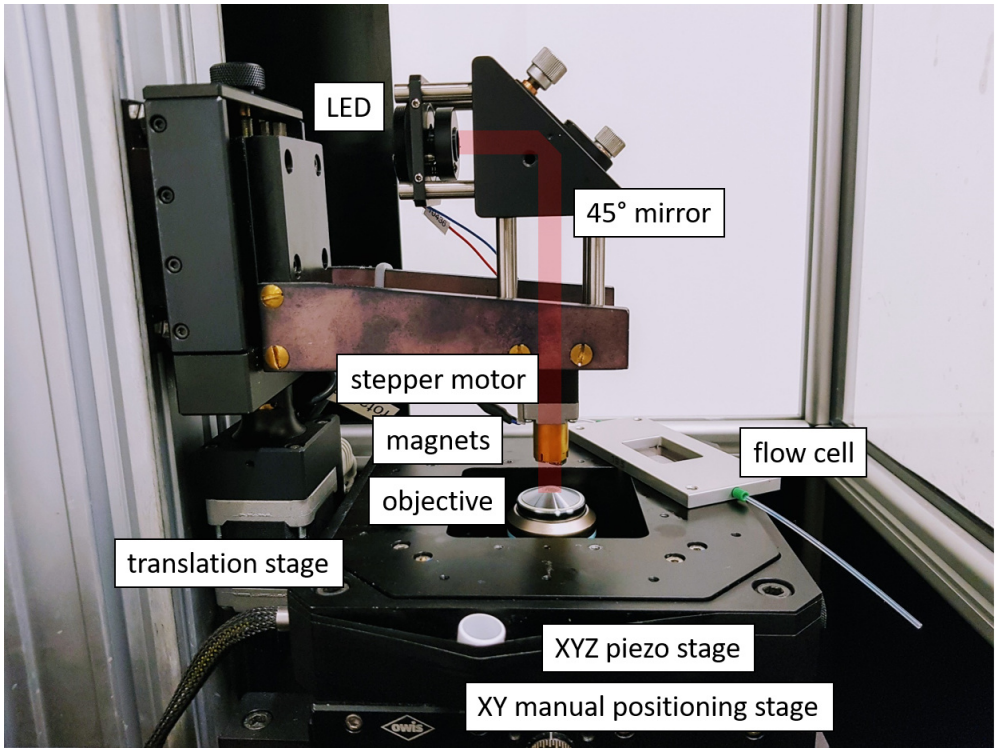

Figure 2.2
The magnetic tweezers setup. A collimated LED is mounted in the kinematic pitch/yaw adapter and coupled into a hollow-shaft stepper motor by a Ø1" mirror. The incoming light passes between a pair of magnets into the objective. The flow cell is mounted on top of an xyz piezo stage, above the objective (here, the flow cell is shifted to the side for clarity). The piezo stage is mounted on top of an xy manual positioning stage, for coarse movements. The magnets and objective are mounted onto two translation stages. Below the objective, the light is coupled into the camera through an infinity-corrected tube lens by means of a Ø2" mirror. The light path is depicted in red.

7. Start tracking the beads (*see* **Notes 36 and 37**).

2.3.7 Force calibration

1. For force calibration, prepare a flow cell containing torsionally free DNA tethers. Preferably, the tethers are relatively long with respect to the magnetic bead size (*see* **Note 38**). Start the measurements with the magnets far away, exerting negligible force. Move the magnets quickly down to the position that needs to be calibrated, keep the magnets fixed for 120 seconds (*see* **Note 39**), and move the magnets upwards. Append two stretches of negligible force before and after the experiment to provide a reference for drift correction. If possible, increase the sample rate f_s of

the camera (*see* **Note 38**). Perform multiple calibration measurements at different magnet positions.

2. Load the data into data analysis software such as LabVIEW, Origin, Python or Excel. Correct the drift by subtracting a term proportional with time from the extension prior to further analysis (*see* **Note 40**).

3. Exclude anomalous events, such as sticking (*see* **Note 41**), double bead attachment to a single tether (*see* **Note 42**), or double tether attachment to a single bead (*see* **Note 43**).

4. Evaluate the x-coordinates (the direction of the magnetic field) in the time-domain where the magnet was exerting a constant force. Compute the single-sided power spectral density (PSD) in units of $\mu m^2_{rms}/Hz$.

5. Exclude all spectral components below 1 Hz, to discard $1/f$ noise and to minimize the effect of drift.

6. Fit the PDS to a blur and aliasing corrected PSD function to obtain the cut-off frequency to calculate the force

$$\mathrm{PDS}_{\mathrm{corrected}}(f, f_c) = \frac{\sigma^2}{f_s} + \sum_{n=-1}^{1} \frac{k_{\mathrm{B}}T}{\gamma\pi^2\left(f_c^2 + (f + nf_s)^2\right)} \left(\frac{\sin\left(W\pi(f + nf_s)\right)}{W\pi(f + nf_s)}\right)^2. \tag{2.1}$$

See **Note 44** for a derivation of Equation 2.1 and a full description of the parameters.

7. Plot force F as a function of magnet position h, and fit the data with a bi-exponential decay [25]

$$F(h) = F_{\max}\left(0.7\exp\left(\frac{-h}{c_1}\right) + 0.3\exp\left(\frac{-h}{c_2}\right)\right). \tag{2.2}$$

This relation is unique for each combination of magnets and the type of magnetic beads. For our setup and 2.8 µm beads, we obtained $F_{\max} = 85$ pN, $c_1 = 1.4$ mm and $c_2 = 0.8$ mm.

2.3.8 Force spectroscopy experiments

1. For a dynamic force spectroscopy experiment on a torsionally free substrate, move the magnets down, increasing the force, and subsequently upwards, releasing the force. Move the magnets at a speed of 0.2 mm/s (*see* **Note 45**). Minimize the dwell time at the highest force to reduce the chance of a tether break. Several variations in trajectories are found in **Note 46**. Optionally, two stretches of low force can be appended before and after the experiment for drift correction.

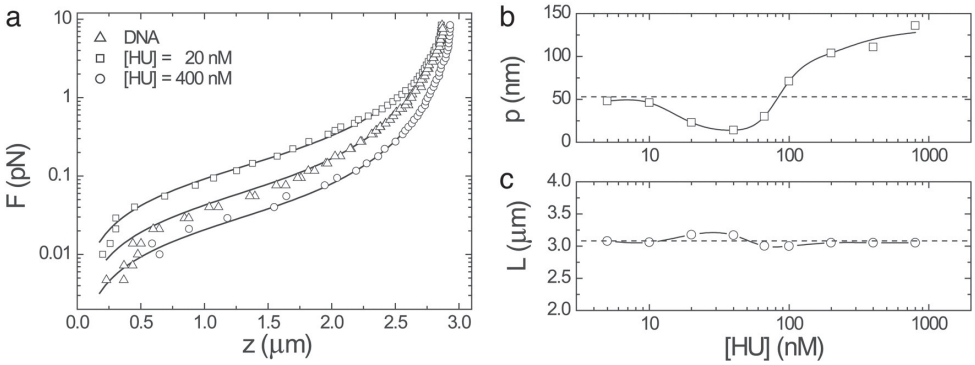

Figure 2.3
The concentration of nucleoid-associated protein HU has a dual effect on the measured stiffness of a DNA tether. (a) The force-extension (F (pN) vs. z (µm)) curves of DNA incubated with increasing concentration of HU. Solid lines represent fits to the extensible WLC model (Equation 2.3). The experiments reveal tether softening at nM HU concentration and tether stiffening at µM HU concentration. Experiments were performed in 60 mM of KCl and 20 mM HEPES (pH 7.9). (b and c) The persistence length p(nm) and contour length L (µm) as a function of HU concentration ([HU] (nm)). The dashed lines represent the values for bare DNA. Individual HU dimers introduce kinks in the DNA at nM HU concentration [35], resulting in a reduced persistence length. A rigid nucleoprotein filament is formed at high HU concentration. HU concentration does not affect the contour length. Reproduced from ref. [6] with permission from PNAS (Copyright (2004) National Academy of Sciences, U.S.A.)

2. For a dynamic force spectroscopy experiment on a torsionally constrained substrate, follow the same procedure as above. Optionally, pre-twist the torsionally constrained substrate before a dynamic force spectroscopy experiment: rotate the magnetic field while the stretching force upon the tether is kept low. Forces as low as 0.05 pN are sufficient for the bead to follow the rotation of the magnetic field. Rotate the magnets with a speed of 2 rotations per second (*see* **Note 47**).

2.3.9 Rotational spectroscopy experiments

1. For rotational spectroscopy on a torsionally constrained substrate, set the force by fixing the magnet height throughout the experiment. Rotate the magnets with a speed of 2 rotations per second. Apply positive twist as desired and relax the tether. Minimize the dwell time at the highest number of rotations (*see* **Note 48**). Apply an equal amount of negative twist at the same rotational speed, and relax the tether. Optionally, two stretches with fixed rotation can be appended before and after the experiment for drift correction.

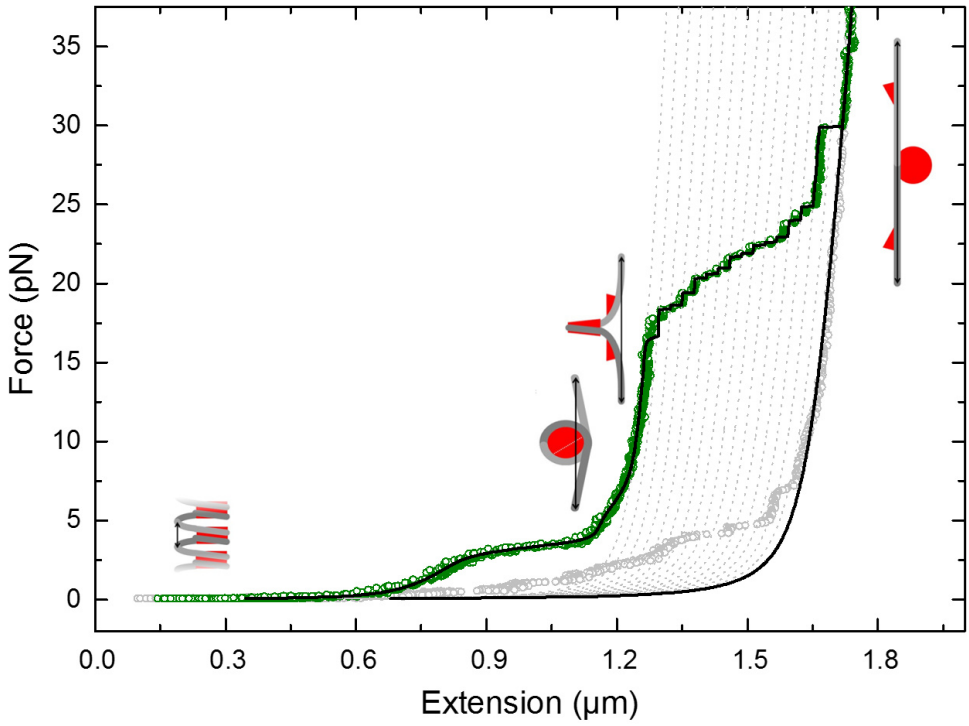

Figure 2.4
Force spectroscopy on a eukaryotic chromatin fiber reveals different levels of compaction in 2 mM $MgCl_2$. The green curve is the stretch curve; the grey curve is the release curve. The black line describes a fit of the data to the statistical mechanics model [11]. The chromatin was reconstituted on an array of 15 Widom 601 nucleosome positioning sequences spaced by 50 base pairs [36]. The low-force regime shows a non-cooperative transition at 3.5 pN, typical for a solenoid chromatin fiber, where the interactions between the nucleosomes are broken and the outer turn of DNA unwraps from the histone core, forming a beads-on-a-string structure. At approximately 6 pN, another transition takes place where this structure is slightly extended. Above 10 pN stepwise unwrapping indicates release of the final wrap of DNA from the histone core. The dashed lines represent discrete 25 nm steps. The chromatin fiber follows the force-extension curve of bare DNA at forces exceeding 25 pN and fits well with an extensible WLC model.

2.3.10 Data analysis of force spectroscopy experiments

1. Load the data into data analysis software such as LabVIEW, Origin, Python or Excel. Calculate force from magnet height using Equation 2.2. Correct the drift by subtracting a term proportional with time from the extension, such that the parts of the extension trace that were appended to the start and the end have the same height (*see* **Note 40**). Alternatively, a (linear) time-dependent term can be included the fitting model. Plot the force as function of extension (*see* **Note 49**).

2. Exclude anomalous events, such as sticking (*see* **Note 41**), double bead attachment to a single tether (*see* **Note 42**), or double tether attachment to a single bead (*see* **Note 43**).

3. Fit the data.

   (a) For bare DNA, fit an extensible WLC model to the data:

   $$z(F,t) = L\left(1 - \frac{1}{2}\sqrt{\frac{k_{\mathrm{B}}T}{FP}} + \frac{F}{S}\right) + z_0 + d \cdot t, \tag{2.3}$$

   where z is the extension, L the contour length, P the persistence length, F the force, S the stretch modulus, k_{B} Boltzmann's constant, T the absolute temperature, and z_0 an offset in extension (*see* **Note 50**). Optionally, a drift, comprising amplitude d and time t can be included.

   (b) For (bacterial) chromatin, fit appropriate models to the data. Generally, the effect of protein binding can be captured in a modified WLC model by adjusting fitting parameters (*see* **Note 51**). An example is shown in Figure 2.3, reproduced from Van Noort *et al.* [6], where the effect of HU-binding on the mechanical parameters of a DNA tether is shown. Analysis of partial nucleoprotein filaments can be performed when the mechanical parameters of homogeneous, fully saturated nucleoprotein filaments have been established. Then, changes in extension can be described as a linear combination of the extensions of parts of bare DNA and parts of nucleoprotein filament [9, 37]. An example of a complex, dynamic chromatin structure is plotted in Figure 2.4, showing force spectroscopy on a nucleosomal array reconstituted from tandem repeats of the Widom 601 sequence and eukaryotic histone proteins [36] (*see* **Note 52**).

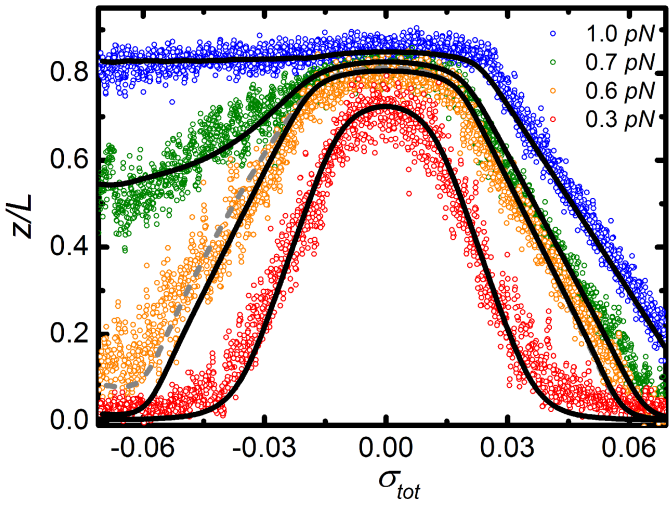

Figure 2.5
The relative extension of a DNA tether as a function of linking number density shows an asymmetric response to twist at forces above 0.5 pN. At low force, plectonemes are formed for both negative and positive twist, reducing the measured extension. Negative twist induces DNA melting at higher force, which keeps the extension constant. The lines represent calculated extensions following a three-state model that distributes twisted, plectonemic and melted regions in the DNA. Reproduced from ref. [31] with permission from Elsevier.

2.3.11 Data analysis of rotational spectroscopy experiments

1. Load the data into data analysis software. Correct the drift following the same procedure as that of the force spectroscopy experiments. Correct the offset in z by computing the first percentile of the extension as a measurement of the surface and subtract it from all z-coordinates. Calculate linking number density from magnet rotation (*see* **Note 53**). Plot the relative extension as a function of linking number density.

2. Exclude disruptive events, following the same procedure as that of the force spectroscopy experiments (*see* **Notes 54-57**).

3. Fit the data.

   (a) For bare DNA, to a three-state model [31], which describes the coexistence of twisted, melted and plectonemic conformational states (*see* **Note 58**). An example is shown in Figure 2.5.

   (b) For (bacterial) chromatin, fit an appropriate model to the data. The torsional response of chromatin fibers can be modeled as a linear combination of twisted and wrapped DNA [38] (*see* **Note 59**).

2.4 Notes

1 Although the torque is proportional to the strength of the magnetic field, the force in MT is proportional to the gradient of the magnetic field and therefore rapidly reduces with distance.

2 In the measurement buffer: HEPES buffers the pH, NaCl sets the ionic strength, TWEEN 20 is a detergent and prevents aggregation of proteins, sodium azide is highly toxic and is added to prevent bacterial growth (when sodium azide is omitted, use sterile solutions or replace buffers frequently), and BSA is used as a crowding agent and retains flow cell passivation. In the passivation buffer, a high concentration of BSA is used to block non-specific binding of DNA and beads and tethers to the surface.

3 For the DNA tethers, we generally use a pUC18-based DNA plasmid, carrying ampicillin resistance. We digest this plasmid with restriction enzymes BsaI and BseYI. For the handles of the torsionally constrained construct, we also use a pUC18 DNA plasmid as a template for PCR. The forward and backward primers were `5' CTC CAA GCT GGG CTG TGT 3'` and `5' GAT AAA TCT GGA GCC GGT GA 3'`. Reconstituted chromatin fibers were made using a plasmid containing 15 repeats of the Widom 601 positioning sequence spaced by 50 base pairs [36].

4 Make LB medium by diluting 10 g tryptone, 10 g NaCl and 5 g yeast extract in 1000 mL Milli-Q water. Make LB agar plates by diluting 10 g tryptone, 10 g NaCl, 5 g yeast extract and 20 g agar in 1000 mL Milli-Q water.

5 We advise to use Invitrogen Dynabeads™ M-270 Streptavidin or MyOne™ Streptavidin T1 paramagnetic beads. These beads have a relatively high iron content (MyOne: 26% / M-270: 14%) and monodispersed size distribution (CV $< 3\%$), which is important for reaching high forces, reliable bead tracking, and force calibration.

6 When handling frozen competent cells, it is important to keep them cool. Frozen cells are very sensitive to temperature and will lose competence if not kept on ice.

7 Very low concentrations, down to picograms per microliter, are sufficient.

8 Use a reaction volume of at least 20 – 50 µL per µg DNA in a digestion.

9 Digestion of (hundreds of) micrograms of DNA plasmid requires overnight incubation. We frequently observe undigested DNA plasmid in agarose gel electrophoresis if we shorten the incubation time.

10 Inactivation temperatures vary for different restriction enzymes.

11 The Promega Wizard SV Gel & PCR cleanup kit uses high concentrations of chaotropic agents to perturb the hydrogen bond network of the solvent, enabling DNA to bind to the silica of the cleanup kit [39–42].

12 Multiple elutions with the spin column improve the yield. Furthermore, a longer incubation time increases the yield. For precious samples, the increased yield outweighs the increased waiting time.

13 This step can be performed longer, up to overnight.

14 Keep the reaction volumes small to reduce costs.

15 The difference between dNTP and ddNTP is that the ddNTP is lacking an OH group at its 3' carbon, which is required for DNA polymerization. It prevents incorporation of more than one affinity tag per DNA strand as the strand cannot be extended.

16 Ethidium bromide is an intercalating agent that fluoresces upon binding to DNA and illumination by a UV light source [43]. To visualize DNA in agarose gels it can be added to the electrophoresis gel or to the running buffer.

17 BseYI can remain bound to DNA after digestion and alter the migration of DNA in agarose gels. To dissociate BseYI, add SDS to a final concentration of 0.5% or purify DNA before agarose gel electrophoresis, for instance with the Promega Wizard SV Gel & PCR cleanup kit.

18 Minimize UV exposure of the sample to prevent DNA damage. Accordingly, block UV exposure of the gel with a non-transparent material such as aluminum foil. Use flanking DNA ladders to estimate the position to cut the DNA fragment from the gel. After cutting, verify that the desired band is cut out by imaging on the UV transilluminator.

19 Dissolving the gel generally results in milliliters of DNA solution. To purify, load the spin column several times. Do not exceed the maximum amount of DNA that can be purified specified for the column.

20 DNA plasmid pUC18 was used as a template for the primers to construct DNA handles.

21 The PCR mixture contains 10% of biotin or digoxigenin labeled dUTP. The PCR product will thus have approximately 10 – 20 affinity tags incorporated.

22 Use labeled dUTPs instead of ddUTPs, since chain termination is undesired.

23 The small digestion products from the ends of the DNA (7 base pairs on the BseYI-side and 32 base pairs on the BsaI-side) are discarded by the Promega Wizard SV Gel & PCR cleanup kit, which has a cut-off at 100 base pairs.

24 The digested pUC18 DNA (with 601-array) is approximately 7 times the length of the digested PCR products. To reach the approximate 1 : 1 : 1 molar ratio, use 1/7 : 1 : 1/7 weight ratio (multi-digoxigenin PCR product : digested pUC18 DNA (with 601-array) : multi-biotin PCR product).

25 The unit definition of T4 DNA ligase can be quite ambiguous. In our protocol we use excessive amounts of T4 ligase for optimal yields.

26 Purifying a DNA construct with multiple affinity tags will strongly reduce the yield as the affinity tags increase DNA adhesion to the column. The yield can be improved by multiple elutions and longer incubation times (up to hours).

27 Mix thoroughly with, for instance, a flattened pipette tip to mix. Upon mixing, the PDMS starts to cure. Higher temperatures accelerate this process.

28 Nitrocellulose coating of the cover slip makes the surface hydrophobic, enhancing AD binding.

29 Incubate the flow cell with a high concentration of BSA to passivate the surface area. This step will reduce sticking of chromatin tethers during experiments.

30 DNA can be replaced by pre-incubated protein-DNA complexes, for instance, reconstituted or native chromatin.

31 During incubation of paramagnetic beads, keep the flow cell upright such that the beads move towards the coated cover slip by gravity.

32 During flushing, turn the flow cell upside down such that unbound beads will detach from the surface.

33 Our MT setup, depicted in Figure 2.2, is home-built and equipped with custom control and tracking software written in LabVIEW (available upon request). A pair of magnets are mounted 0.8 mm apart, at the center axis of a hollow shaft stepper motor that is mounted on a stepper motor-actuated translation stage. The magnets are oriented with their magnetization axis vertically, in opposite directions. For proper orientation, ensure that the magnets attract each other yet do not allow

rotation around the axis connecting the centers of the magnets. The microscope objective is mounted on a stepper motor-actuated translation stage to allow for coarse focusing. Stepper motors are controlled by a 6-axis two-phase stepper motor driver. A collimated LED is mounted in a kinematic pitch/yaw adapter above the hollow shaft motor, and provides a homogeneous illumination of the flow cell. We use an inverted microscope layout, including a tube lens and monochrome camera, to record the out-of-focus images of the Lorentz–Mie scattering pattern of the tethered bead [44]. The flow cell is mounted on an xyz piezo stage, for accurate control of the focus position. The xyz piezo stage is mounted onto an xy positioning stage, for manual coarse translation of the flow cell. The microscope setup is surrounded by a box to minimize acoustic and thermal fluctuations and to protect the setup from dust.

34 Before each experiment, the focus should be adjusted so that we always measure in the same plane.

35 An automatic bead finder algorithm is currently implemented, which cross-correlates the field-of-view with a computer-generated reference image that resembles the beads. Beads are selected by setting a threshold on the cross-correlation amplitude.

36 During a typical measurement, a series of frames are acquired and processed in real-time. The magnet position and rotation are recorded in synchrony by the same software that controls the frame grabber. Data collection is buffered in two parallel processes:

(a) **Image acquisition.** The camera captures full frames at a speed of 30 fps. The assigned ROIs and frame numbers are extracted and stored in a buffer.

(b) **Image analysis.** In parallel, the buffer is read out and analyzed. Each ROI is cross-correlated with a set of computer-generated reference images, using a FFT-based correlation algorithm. The maximum of the cross-correlation represents the xy-coordinates of the bead and is determined with sub-pixel accuracy. The phase of the cross-correlation at this location is also extracted, converted to a z-coordinate and written into a binary file. From the frame number and camera frequency a time column is computed and stored in the same file. After each measurement, the binary file is transformed into an ASCII-file that allows for versatile data processing. This file contains a time column, a column with the motor positions and four columns per bead: three spatial coordinates and the amplitude of the cross-correlation.

37 Any appropriate bead tracking algorithm will suffice for this step. Use, for instance, the cross-correlation method [45], a center-of-mass calculation [46], directly fitting a Gaussian curve to the intensity profile [47], the quadrant-interpolation method [48] or the phase tracking method (introduced in Chapter 3 of this thesis).

38 We used a 6955 base pairs DNA tether ($\sim$ 2.4 µm) to calibrate 1.0 µm and 2.8 µm diameter magnetic beads and recorded images with a frame rate of 200 Hz. Longer tethers provide a better signal-to-noise ratio, therefore, it is not uncommon that Lambda-DNA is used for calibration, which is 48,502 base pairs ($\sim$ 16.5 µm) in length. If appropriate camera corrections are applied (*i.e.* motion blur and aliasing, *see* **Note 44**), force calibration can be performed with shorter tethers.

39 The required measurement time τ_m for a desired statistical accuracy ϵ is described in Equations 2.4 and 2.5 [25]

$$\tau_m \approx \frac{12\pi^2\eta RL}{F\epsilon^2} \qquad \text{for } F > 1 \text{ pN}, \tag{2.4}$$

$$\tau_m \approx \frac{8\pi^2\eta RPL}{k_{\mathrm{B}}T\epsilon^2} \qquad \text{for } F < 1 \text{ pN}, \tag{2.5}$$

where η is the viscosity of water, R the radius of the bead, L the DNA contour length, F the calibrated force, and P the persistence length. Typically, the statistical accuracy ϵ is set to 0.05. We measure each magnet position for 120 seconds, which is well within limits.

40 A plot of extension as a function of time may reveal drift as a steady increase or decrease of extension over time. When beginning and ending a trajectory at low force (or no rotations), at which the z-position of the bead is constrained by the bottom slide of the flow cell, compare the first percentile of the bead height of these two segments to quantify the drift. Calculate the first percentile rather than the average, since the surface poses a one-sided boundary to the bead motion. The first percentile will give a good estimation of the surface position, which is required for drift characterization. Typically, we measure less than 1 nm/s drift of the extension, yet this can accumulate to signification deviations of the measured force-extension curves.

41 When the bead is in close proximity to the surface, non-specific interactions between the bead and the surface can cause the bead or part of the tether to stick to the flow cell bottom, immobilizing the bead. Small forces are generally sufficient to unstick the bead and resume the measurement as normal. As opposed to intramolecular rupturing or folding events, (un-)sticking events can be identified in the data as an abrupt step in the coordinates in three dimensions, rather than only in the z-direction.

42 A double bead doubles the force exerted on the tether, therefore, transitions are measured at half the force at which they are expected (for instance, DNA overstretching measured at half the force). The measured persistence length is double of that measured with a single bead. Furthermore, the data is generally very noisy, since tracking becomes problematic with two beads in the same ROI.

43 A double tether halves the force exerted on the tether. Therefore, transitions are measured at double the force as they are expected and add up (for instance, double the amount of stepwise unwrapping events when stretching chromatin, measured at double the force). The measured persistence length is half that of a single tether. A plot of the x-coordinates versus the y-coordinates of the bead during drift characterization is asymmetric.

44 The magnetic force pulls the tethered bead in the z-direction and is counteracted by a restoring force from the tether. Brownian motion causes the bead to move away from its central position. The potential energy $E_p(x)$ in the direction of the field (x-direction) around the equilibrium position is described by:

$$E_p(x) = \frac{1}{2} k_x \delta x^2, \tag{2.6}$$

where δx^2 is the variance of the bead fluctuations. The effective trap stiffness k_x follows

$$k_x = \frac{F}{z}, \tag{2.7}$$

where F is the stretching force and z the bead height. The equipartition theorem states that the energy per degree of freedom equals $\frac{1}{2} k_\mathrm{B} T$. The force therefore follows

$$F = \frac{k_\mathrm{B} T z}{\langle \delta x^2 \rangle}. \tag{2.8}$$

For an accurate experimental determination of the force however, it is necessary to look into the frequency f dependence of the thermal fluctuations of x. Start by computing the PSD in the direction of the field at constant force. Since the PDS follows a Lorentzian curve

$$\mathrm{PDS}_\mathrm{thermal}(f, f_c) = \frac{k_\mathrm{B} T}{\gamma \pi^2 (f_c^2 + f^2)}, \tag{2.9}$$

which is fully defined by the lateral friction coefficient γ and the cut-off frequency f_c

$$f_c = k_x / 2\pi\gamma. \tag{2.10}$$

The friction coefficient γ depends on the bead radius R and the viscosity η (which increases with closer proximity to the surface, *see* **Note 60**)

$$\gamma = 6\pi\eta R, \tag{2.11}$$

resulting, together with equation 7, in

$$F = 12\pi^2 \eta R z f_c. \tag{2.12}$$

Thus, fitting f_c from the PDS yields the force for a given magnet position. However, the finite integration time of the camera averages out some of the bead's movement, an effect known as blurring. To account for blurring, a correction term C_{blur} must be applied [24–26, 49, 50]:

$$C_{\text{blur}} = \left(\frac{\sin(W\pi f)}{W\pi f} \right)^2, \tag{2.13}$$

where W is the frame integration time. The finite sampling frequency of the camera causes another artefact, known as aliasing. Aliasing can be described by folding back the parts of the spectrum that exceed the sampling frequency f_s

$$\text{PDS}_{\text{alias}}(f, f_c) = \sum_n \text{PDS}_{\text{thermal}}(f + nf_s, f_c) C_{\text{blur}}(f + nf_s). \tag{2.14}$$

It usually sufficient to include only one aliasing term, *i.e.* $n = -1...1$ [24]. Finally, the PSD is offset by a tracking error of variance σ^2 that is independent of frequency [50]

$$\text{PDS}_{\text{tracking}} = \frac{\sigma^2}{f_s}, \tag{2.15}$$

in which f_s is the sampling frequency. Overall, fitting

$$\text{PDS}_{\text{corrected}}(f, f_c) = \frac{\sigma^2}{f_s} + \sum_{n=-1}^{1} \frac{k_{\text{B}}T}{\gamma\pi^2 \left(f_c^2 + (f + nf_s)^2\right)} \left(\frac{\sin\left(W\pi(f + nf_s)\right)}{W\pi(f + nf_s)} \right)^2. \tag{2.16}$$

to the experimental spectrum of the lateral fluctuations will yield the cut-off frequency which is used to calculate the force. Equation 2.16 is the same expression as Equation 2.1.

45 The loading rate increases exponentially with magnet speed. For forces below 5 pN, we typically have a loading rate that ranges between 0 - 0.75 pN/s. High loading rates shift the rate of non-equilibrium events such as breaking of bonds between antibodies [51].

46 Several variations of magnet trajectories can be used:

(a) Repeat loops to gain insight into the reversibility of DNA folding.

(b) To approach a linear loading rate, break up the trajectory in several segments with decreasing magnet speeds.

(c) Start with a short force ramp up to 0.5 pN to set free loosely stuck beads.

47 Torsionally constrained substrates build up torque while stretched, and consequently respond differently to force. These substrates can be pre-twisted before an experiment to study the role of supercoiling. DNA compacted by histone-like proteins for instance has an intrinsically twisted structure.

48 Supercoiling reduces the bead height, which increases the probability of beads or tethers to stick to the surface. Minimizing the dwell time at the maximum number of rotations reduces sticking.

49 Plot force as function of extension. Plotting it in this way is customary for optical tweezers and allows for easy comparison between methods. Because MT form a force clamp rather than a position clamp, this way of plotting may be counterintuitive.

50 For tethers that have a length that is in range with the size of the bead, off-center attachment of the DNA to the bead may lead to a large error in the measured extension. Super-paramagnetic beads have a small, but finite permanent magnetic moment, giving them a preferred orientation when exposed to a magnetic field [52]. Since tethering happens in the absence of the magnetic field, application of force will turn the magnetic moment in the direction of the magnetic field, typically horizontally, while maximizing the height of the bead. When the DNA is attached at a location exactly at the circumference of the bead that has equal distance between the magnetic poles, it will rotate the bead, such that the attachment point will be at the bottom of the bead. Any location remote from this circle will still rotate the bead around the horizontal axis along the poles, but cannot spin the bead along the horizontal axis perpendicular to the poles. Consequently, there will be an offset between the height of the bead and the extension of the tether, and the measured extension is underestimated. This artefact is specific for MT and can be corrected by shifting the data in the z-direction, or by including this offset as a fitting parameter.

51 Specific modes of protein binding yield distinctive patterns:

(a) Coating the DNA tether yields a stiffening of the DNA, which can be parameterized by an increased persistence length in the entropic regime at low force and/or and increased stretch modulus at high force. These two effects can only be differentiated when a large force range is probed. Examples are HU (at µM concentration) [6] and H-NS (at nM concentration) [9, 53, 54].

(b) Bending induces a kink in the DNA trajectory, which is apparent as a reduced persistence length [35]. The magnitude of this reduction scales with the kink angle and the number of kinks, which reflect the structure and number of proteins bound to the tether. Examples of chromatin proteins that introduce a kink are HU (at nM concentration) [6, 55] and IHF (at nM concentration) [56].

(c) Wrapping of DNA around proteins results in both a reduction of the persistence length, similar to bending and depending on the amount of DNA that is wrapped, and a reduction of the contour length. When exactly 1 wrap is formed, the persistence length is similar to that of bare DNA. The archetype of wrapping proteins is the eukaryotic histone octamer that wraps 1.7 turns of DNA [57–59]. Archaeal histones wrap smaller DNA lengths [60, 61].

(d) Bridging involves protein-induced formation of contacts between distant part of the DNA tether and results in a large reduction of the contour length. The DNA that is captured in the loop does not contribute to the extension of the tether. An examples of a bridging protein is H-NS, whose mode of binding depends on the concentration of monovalent and divalent ions [9, 53, 54].

(e) Stabilization of single-stranded DNA. Melting parts of the dsDNA tether by force and or torque yields sections of single stranded DNA. This leads to a 1.6 times extension of the contour length, as well as a reduction of the persistence length down to a few nanometers in absence of protein covering the single-strand DNA [37]. Single-strand binding proteins like SSB prevent annealing of force-induced, melted DNA, yielding force-extension curves that display a large hysteresis [62].

52 Various force regimes reveal different chromatin conformations that can all be captured in a force-dependent linear combination of bare DNA and 4 different nucleosome structures [11]. Bacterial chromatin typically consists of proteins that bend, rather than wrap DNA, have a smaller footprint and are usually interspersed with different types proteins. Furthermore, they may have more varying sequence preferences. Nevertheless, a similar analysis, customized for different characteristics of individual proteins, can be used to retrieve a detailed understanding of chromatin folding based on force spectroscopy. When the chromatin conformation is not stable due to changes of protein concentration, force or salt, this may result in a change in extension. From such changes it is possible to extract binding and/or dissociation rates.

53 Calculate the linking number density, using $\sigma = \Delta Lk/Lk_0$, where Lk_0 is the linking number of DNA and equals the contour length in base pairs

divided by the helical pitch of DNA, which is 10.4 base pairs. The change in linking number, ΔLk, equals the number of rotations of the magnets.

54 A double bead affects rotational spectroscopy measurements similar to force spectroscopy measurements. The tether is more likely to break since the force that is kept constant during the measurement is double of that expected.

55 A double tether inhibits rotational spectroscopy measurements similar to force spectroscopy measurements. Double tethers can easily be identified when twisting the tether. During the first turn, the bead is pulled down by a large step, as the two molecules get braided. Subsequent twist lowers the bead for both negative and positive rotations, as opposed to single tethers, for which the extension is independent of negative twist at forces exceeding 1 pN.

56 The DNA tether can become nicked during sample preparation. A single nick is sufficient to release torque and consequently the tether cannot be used for rotational spectroscopy. These tethers can be discarded during an initial rotation experiment, or can serve as control for torsionally unconstraint tethers.

57 Plot all x-coordinates versus all y-coordinates during rotation of the bead. The shape of this plot should describe a circle. The radius of the circle equals the attachment offset from the center of the bead.

58 Since mechanical properties of twisted DNA are much more complex than those of torsionally free DNA, fitting the curves is challenging. The three-state model developed by Meng *et al.* [31] describes the coexistence of twisted, melted and plectonemic conformational states. The data and the model feature symmetric buckling at low forces ($F < 0.6$ pN), where both positive and negative twist is absorbed by plectonemes. At higher forces ($F > 0.6$ pN) the extension-twist curve becomes asymmetric, and negative twist is absorbed by local melting of the DNA.

59 Quantitative analysis of the torsional stress in chromatin filaments is more involved. Bending proteins (such as HU of IHF) and wrapping proteins (such as HMf or eukaryotic histones) induce writhe in a torsionally constrained tether, while twist remains constant. The torsional stiffness of such fibers has not been measured, though quantification is highly desirable to test proposed models of twist-induced (de-)compaction of chromatin fibers and their role in transcription regulation. Eukaryotic tetrasomes have been shown to have a complex dynamic chirality [28, 29].

60 Beads experience an increasing viscosity as the distance to the surface approaches the bead diameter [63]. The height dependence of the lat-

eral friction coefficient γ is approximated by Faxén's law, described in Equation 2.17.

$$\gamma = \frac{\gamma_0}{1 - \frac{9R}{16h} + \frac{R^3}{8h^3} - \frac{45R^4}{256h^4} - \frac{R^5}{16h^3}} \tag{2.17}$$

where $\gamma_0 = 6\pi\eta R$ is the bulk friction coefficient, η the viscosity, R the radius of the bead, and h the distance of the bead center to the surface.

Bibliography II

[1] Martijn S Luijsterburg et al. "The major architects of chromatin: architectural proteins in bacteria, archaea and eukaryotes". In: *Critical reviews in biochemistry and molecular biology* 43.6 (2008), pp. 393–418.

[2] Carlos Bustamante, Zev Bryant, and Steven B. Smith. "Ten years of tension: single-molecule DNA mechanics". In: *Nature* 421.6921 (2003), pp. 423–427. ISSN: 0028-0836. DOI: 10.1038/nature01405.

[3] S. Smith, L Finzi, and C Bustamante. "Direct mechanical measurements of the elasticity of single DNA molecules by using magnetic beads". In: *Science* 258.5085 (1992), pp. 1122–1126. ISSN: 0036-8075. DOI: 10.1126/science.1439819.

[4] T. R. Strick et al. "The elasticity of a single supercoiled DNA molecule." In: *Science (New York, N.Y.)* 271.5257 (1996), pp. 1835–1837. ISSN: 0036-8075. DOI: 10.1126/science.271.5257.1835.

[5] Charlie Gosse and Vincent Croquette. "Magnetic tweezers: micromanipulation and force measurement at the molecular level." In: *Biophysical Journal* 82.6 (2002), pp. 3314–3329. ISSN: 0006-3495. DOI: 10.1016/S0006-3495(02)75672-5.

[6] J. van Noort et al. "Dual architectural roles of HU: Formation of flexible hinges and rigid filaments". In: *Proceedings of the National Academy of Sciences* 101.18 (2004), pp. 6969–6974. ISSN: 0027-8424. DOI: 10.1073/pnas.0308230101.

[7] Marijn T J Van loenhout et al. "Dynamics of RecA filaments on single-stranded DNA". In: *Nucleic Acids Research* 37.12 (2009), pp. 4089–4099. ISSN: 03051048. DOI: 10.1093/nar/gkp326.

[8] Timothée Lionnet et al. "Single-molecule studies using magnetic traps". In: *Cold Spring Harbor Protocols* 7.1 (2012), pp. 34–49. ISSN: 19403402. DOI: 10.1101/pdb.top067488.

[9] Ci Ji Lim, Linda J. Kenney, and Jie Yan. "Single-molecule studies on the mechanical interplay between DNA supercoiling and H-NS DNA architectural properties". In: *Nucleic Acids Research* 42.13 (2014), pp. 8369–8378. ISSN: 13624962. DOI: 10.1093/nar/gku566.

[10] Ramon A Van Der Valk et al. "Genomic looping: a key principle of chromatin organization". In: *Journal of molecular microbiology and biotechnology* 24.5-6 (2014), pp. 344–359.

[11] He Meng, Kurt Andresen, and John van Noort. "Quantitative analysis of single-molecule force spectroscopy on folded chromatin fibers". In: *Nucleic Acids Research* 43.7 (Apr. 2015), pp. 3578–3590. ISSN: 13624962. DOI: 10.1093/nar/gkv215.

[12] Jie Yan, Dunja Skoko, and John F. Marko. "Near-field-magnetic-tweezer manipulation of single DNA molecules". In: *Physical Review E - Statistical, Nonlinear, and Soft Matter Physics* 70.1 1 (2004). ISSN: 15393755. DOI: 10.1103/PhysRevE.70.011905.

[13] Bojk A. Berghuis et al. "High-throughput, high-force probing of DNA-protein interactions with magnetic tweezers". In: *Methods* 105 (2016), pp. 90–98. ISSN: 10959130. DOI: 10.1016/j.ymeth.2016.03.025.

[14] Noah Ribeck and Omar A. Saleh. "Multiplexed single-molecule measurements with magnetic tweezers". In: *Review of Scientific Instruments* 79.9 (2008). ISSN: 00346748. DOI: 10.1063/1.2981687.

[15] Iwijn De Vlaminck et al. "Highly parallel magnetic tweezers by targeted DNA tethering". In: *Nano Letters* 11.12 (2011), pp. 5489–5493. ISSN: 15306984. DOI: 10.1021/nl203299e.

[16] Jan Lipfert et al. "Freely orbiting magnetic tweezers to directly monitor changes in the twist of nucleic acids." In: *Nature communications* 2.May (2011), p. 439. ISSN: 2041-1723. DOI: 10.1038/ncomms1450. arXiv: arXiv:1011.1669v3.

[17] Jan Lipfert et al. "Magnetic torque tweezers: measuring torsional stiffness in DNA and RecA-DNA filaments". In: *Nature Methods* 7.12 (Oct. 2010), pp. 977–980. ISSN: 1548-7091. DOI: 10.1038/nmeth.1520.

[18] J. K. Fisher et al. "Thin-foil magnetic force system for high-numerical-aperture microscopy". In: *Review of Scientific Instruments* 77.2 (2006). ISSN: 00346748. DOI: 10.1063/1.2166509.

[19] Piercen M. Oliver, Jin Seon Park, and Dmitri Vezenov. "Quantitative high-resolution sensing of DNA hybridization using magnetic tweezers with evanescent illumination". In: *Nanoscale* 3.2 (2011), pp. 581–591. ISSN: 2040-3364. DOI: 10.1039/C0NR00479K.

[20] John S. Graham, Reid C. Johnson, and John F. Marko. "Concentration-dependent exchange accelerates turnover of proteins bound to double-stranded DNA". In: *Nucleic Acids Research* 39.6 (2011), pp. 2249–2259. ISSN: 03051048. DOI: 10.1093/nar/gkq1140.

[21] John S. Graham, Reid C. Johnson, and John F. Marko. "Counting proteins bound to a single DNA molecule". In: *Biochemical and Biophysical Research Communications* 415.1 (2011), pp. 131–134. ISSN: 0006291X. DOI: 10.1016/j.bbrc.2011.10.029. arXiv: NIHMS150003.

[22] Xi Long et al. "Mechanical unfolding of human telomere G-quadruplex DNA probed by integrated fluorescence and magnetic tweezers spectroscopy". In: *Nucleic Acids Research* 41.4 (2013), pp. 2746–2755. ISSN: 03051048. DOI: 10.1093/nar/gks1341.

[23] ID Vilfan et al. "Magnetic tweezers for single-molecule experiments". In: *Handbook of Single-Molecule Biophysics*. Springer, 2009, pp. 371–395.

[24] Aartjan J.W. W Te Velthuis et al. "Quantitative guidelines for force calibration through spectral analysis of magnetic tweezers data". In: *Biophysical Journal* 99.4 (2010), pp. 1292–1302. ISSN: 00063495. DOI: 10.1016/j.bpj.2010.06.008.

[25] Zhongbo Yu et al. "A force calibration standard for magnetic tweezers". In: *Review of Scientific Instruments* 85.12 (2014). ISSN: 10897623. DOI: 10.1063/1.4904148.

[26] Peter Daldrop et al. "Extending the range for force calibration in magnetic tweezers". In: *Biophysical Journal* 108.10 (2015), pp. 2550–2561. ISSN: 15420086. DOI: 10.1016/j.bpj.2015.04.011.

[27] Pooja Gupta, Jordanka Zlatanova, and Miroslav Tomschik. "Nucleosome assembly depends on the torsion in the DNA molecule: A magnetic tweezers study". In: *Biophysical Journal* 97.12 (2009), pp. 3150–3157. ISSN: 15420086. DOI: 10.1016/j.bpj.2009.09.032.

[28] Rifka Vlijm et al. "Nucleosome assembly dynamics involve spontaneous fluctuations in the handedness of tetrasomes". In: *Cell Reports* 10.2 (2015), pp. 216–225. ISSN: 22111247. DOI: 10.1016/j.celrep.2014.12.022.

[29] Rifka Vlijm et al. "Comparing the assembly and handedness dynamics of (H3.3-H4)2 tetrasomes to canonical tetrasomes". In: *PLoS ONE* 10.10 (2015). ISSN: 19326203. DOI: 10.1371/journal.pone.0141267.

[30] M. Kruithof et al. "Subpiconewton dynamic force spectroscopy using magnetic tweezers." In: *Biophysical journal* 94.6 (2008), pp. 2343–2348. ISSN: 00063495. DOI: 10.1529/biophysj.107.121673.

[31] He Meng et al. "Coexistence of Twisted, Plectonemic, and Melted DNA in Small Topological Domains". In: *Biophysical Journal* 106.5 (2014), pp. 1174–1181. ISSN: 00063495. DOI: 10.1016/j.bpj.2014.01.017.

[32] John F. Marko and Eric D. Siggia. "Stretching DNA". In: *Macromolecules* 28.26 (Dec. 1995), pp. 8759–8770. ISSN: 15205835. DOI: 10.1021/ma00130a008.

[33] C Bustamante et al. "Single-molecule studies of DNA mechanics". In: *Current opinion in structural biology* 10.3 (June 2000), pp. 279–85. ISSN: 0959-440X. DOI: 10.1016/S0959-440X(00)00085-3.

[34] John F. Marko. "Torque and dynamics of linking number relaxation in stretched supercoiled DNA". In: *Physical Review E - Statistical, Nonlinear, and Soft Matter Physics* 76.2 (2007), pp. 1–13. ISSN: 15393755. DOI: 10.1103/PhysRevE.76.021926.

[35] Igor M. Kulić et al. "Equation of state of looped DNA". In: *Physical Review E - Statistical, Nonlinear, and Soft Matter Physics* 75.1 (2007). ISSN: 15393755. DOI: 10.1103/PhysRevE.75.011913. arXiv: 0509003 [q-bio].

[36] P T T Lowary and J Widom. "New DNA sequence rules for high affinity binding to histone octamer and sequence-directed nucleosome positioning." In: *Journal of molecular biology* 276.1 (1998), pp. 19–42. ISSN: 0022-2836. DOI: 10.1006/jmbi.1997.1494. eprint: NIHMS150003.

[37] Steven B. Smith, Yujia Cui, and Carlos Bustamante. "Overstretching B-DNA: the elastic response of individual double-stranded and single-stranded DNA molecules". In: *Science* 271.5250 (1996), pp. 795–798. ISSN: 0036-8075. DOI: 10.1126/science.271.5250.795. eprint: arXiv:1011.1669v3.

[38] Aurélien Bancaud et al. "Nucleosome Chiral Transition under Positive Torsional Stress in Single Chromatin Fibers". In: *Molecular Cell* 27.1 (2007), pp. 135–147. ISSN: 10972765. DOI: 10.1016/j.molcel.2007.05.037. arXiv: 0708.0156.

[39] Carton W. Chen and Charles A. Thomas. "Recovery of DNA segments from agarose gels". In: *Analytical Biochemistry* 101.2 (1980), pp. 339–341. ISSN: 10960309. DOI: 10.1016/0003-2697(80)90197-9.

[40] M. A. Marko, R. Chipperfield, and H. C. Birnboim. "A procedure for the large-scale isolation of highly purified plasmid DNA using alkaline extraction and binding to glass powder". In: *Analytical Biochemistry* 121.2 (1982), pp. 382–387. ISSN: 10960309. DOI: 10.1016/0003-2697(82)90497-3.

[41] Rene´ Boom et al. "Rapid and Simple Method for Purification of Nucleic Acids". In: *Journal of Clinical Microbiology* 28.3 (1990), pp. 495–503. ISSN: 0910-6340. DOI: 10.2116/analsci.25.941.

[42] Giovanni Salvi, Paolo De Los Rios, and Michele Vendruscolo. "Effective interactions between chaotropic agents and proteins". In: *Proteins: Structure, Function and Genetics* 61.3 (2005), pp. 492–499. ISSN: 08873585. DOI: 10.1002/prot.20626.

[43] J B LePecq and C Paoletti. "A fluorescent complex between ethidium bromide and nucleic acids. Physical-chemical characterization." In: *Journal of molecular biology* 27.1 (1967), pp. 87–106. ISSN: 00222836. DOI: 10.1016/0022-2836(67)90353-1.

[44] Sang-Hyuk Lee et al. "Characterizing and tracking single colloidal particles with video holographic microscopy." In: *Optics express* 15.26 (2007), pp. 18275–18282. ISSN: 1094-4087. DOI: 10.1364/OE.15.018275. arXiv: 0712.1738.

[45] Jeff Gelles, Bruce J. Schnapp, and Michael P. Sheetz. "Tracking kinesin-driven movements with nanometre-scale precision." In: *Nature* 331.6155 (1988), pp. 450–453. ISSN: 0028-0836. DOI: 10.1038/331450a0. arXiv: arXiv:1011.1669v3.

[46] G M Lee, A Ishihara, and K Jacobson. "Direct observation of brownian motion of lipids in a membrane." In: *Proceedings of the National Academy of Sciences of the United States of America* 88.14 (1991), pp. 6274–8. ISSN: 0027-8424. DOI: 10.1073/pnas.88.14.6274.

[47] Catherine M Anderson et al. "Tracking of cell surface receptors by fluorescence digital imaging microscopy using a charge-coupled device camera. Low-density lipoprotein and influenza virus receptor mobility at 4 degrees C." In: *Journal of cell science* 101 (Pt 2 (1992), pp. 415–425. ISSN: 0021-9533.

[48] Marijn T.J. J Van Loenhout et al. "Non-bias-limited tracking of spherical particles, enabling nanometer resolution at low magnification". In: *Biophysical Journal* 102.10 (2012), pp. 2362–2371. ISSN: 00063495. DOI: 10.1016/j.bpj.2012.03.073.

[49] Wesley P Wong and Ken Halvorsen. "The effect of integration time on fluctuation measurements: calibrating an optical trap in the presence of motion blur". In: *Optics express* 14.25 (2006), pp. 12517–31. ISSN: 1094-4087. DOI: 10.1364/OE.14.012517. arXiv: 0607156 [physics].

[50] Astrid van der Horst and Nancy R Forde. "Power spectral analysis for optical trap stiffness calibration from high-speed camera position detection with limited bandwidth." In: *Optics express* 18.8 (2010), pp. 7670–7677. ISSN: 1094-4087. DOI: 10.1364/OE.18.007670.

[51] Gerrit Sitters et al. "Acoustic force spectroscopy." In: *Nature methods* 12.1 (2015), pp. 47–50. ISSN: 1548-7105. DOI: 10.1038/nmeth.3183.

[52] Daniel Klaue and Ralf Seidel. "Torsional stiffness of single superparamagnetic microspheres in an external magnetic field". In: *Physical Review Letters* 102.2 (2009), pp. 1–4. ISSN: 00319007. DOI: 10.1103/PhysRevLett.102.028302.

[53] Yingjie Liu et al. "A divalent switch drives H-NS/DNA-binding conformations between stiffening and bridging modes". In: *Genes and Development* 24.4 (2010), pp. 339–344. ISSN: 08909369. DOI: 10.1101/gad.1883510.

[54] Ramon A van der Valk et al. "Mechanism of environmentally driven conformational changes that modulate H-NS DNA bridging activity". In: *eLife* 6 (2017). ISSN: 2050-084X. DOI: 10.7554/eLife.27369.

[55] Kerren K. Swinger and Phoebe A. Rice. *IHF and HU: Flexible architects of bent DNA*. 2004. DOI: 10.1016/j.sbi.2003.12.003.

[56] Jie Lin et al. "Physical Organization of DNA by Multiple Non-Specific DNA-Binding Modes of Integration Host Factor (IHF)". In: *PLoS ONE* 7.11 (2012). ISSN: 19326203. DOI: 10.1371/journal.pone.0049885.

[57] K Luger et al. "Crystal structure of the nucleosome core particle at 2.8 A resolution." In: *Nature* 389.6648 (1997), pp. 251–260. ISSN: 0028-0836. DOI: 10.1038/38444. arXiv: NIHMS150003.

[58] Thomas Schalch et al. "X-ray structure of a tetranucleosome and its implications for the chromatin fibre". In: *Nature* 436.7047 (2005), pp. 138–141. ISSN: 0028-0836. DOI: 10.1038/nature03686.

[59] F. Song et al. "Cryo-EM Study of the Chromatin Fiber Reveals a Double Helix Twisted by Tetranucleosomal Units". In: *Science* 344.6182 (2014), pp. 376–380. ISSN: 0036-8075. DOI: 10.1126/science.1251413.

[60] Bram Henneman and Remus T. Dame. "Archaeal histones: dynamic and versatile genome architects". In: *AIMS Microbiology* 1.1 (2015), pp. 72–81. ISSN: 2471-1888. DOI: 10.3934/microbiol.2015.1.72.

[61] Francesca Mattiroli et al. "Structure of histone-based chromatin in Archaea". In: *Science* 357.6351 (2017), pp. 609–612. ISSN: 0036-8075. DOI: 10.1126/science.aaj1849.

[62] K. Hatch et al. "Measurement of the salt-dependent stabilization of partially open DNA by Escherichia coli SSB protein". In: *Nucleic Acids Research* 36.1 (2008), pp. 294–299. ISSN: 03051048. DOI: 10.1093/nar/gkm1014.

[63] Erik Schäffet, Simon F. Nørrelykke, and Jonathon Howard. "Surface forces and drag coefficients of microspheres near a plane surface measured with optical tweezers". In: *Langmuir* 23.7 (2007), pp. 3654–3665. ISSN: 07437463. DOI: 10.1021/la0622368.